

Ultra Diffuse Dwarf Galaxies Hosting Pseudo-bulges

YU RONG,^{1,2} HONG-XIN ZHANG,^{1,2} CHENG CHENG,³ QI GUO,³ WEIYU DING,^{1,2} ZICHEN HUA,^{1,2} HUIYUAN WANG,^{1,2} AND XU KONG^{1,2}

¹*Department of Astronomy, University of Science and Technology of China, Hefei, Anhui 230026, China*

²*School of Astronomy and Space Sciences, University of Science and Technology of China, Hefei 230026, Anhui, China*

³*National Astronomical Observatories, Chinese Academy of Sciences, Beijing 100012, China*

ABSTRACT

By analyzing data from DESI Legacy Imaging Survey of the dwarf galaxies in the Arecibo Legacy Fast Alfa Survey, we have identified five ultra-diffuse galaxies (UDGs) featuring central pseudo-bulges. These UDGs display blue pseudo-bulges with Sérsic indices $n < 2.5$ and effective radii spanning 300-700 pc, along with bluer thin stellar disks exhibiting low surface brightness and expansive effective radii that align with the UDG definition. The rotation velocities of these UDGs, determined using HI line widths and optical inclinations, exceed those of most dwarf galaxies of similar mass, suggesting the high halo spins or substantial dark matter halos. We propose that these UDGs likely formed through mergers of dwarf galaxies lacking old stars in their progenitors, resulting in the development of central bulge-like structures during starbursts triggered by the mergers, while also enhancing their halo spin. Subsequent gas accretion facilitated the formation of extended stellar disks. It is also worth noting the possibility that these UDGs could alternatively represent “failed L^* galaxies” with massive dark matter halos but reduced star formation efficiencies. If future high-resolution HI observations confirm the presence of massive halos around these UDGs, they may have formed due to intense AGN feedback in the early universe, and may be the descendants of “little red dots” observed by the James Webb Space Telescope, which are characterized by heightened central black hole masses and intensified accretion and feedback processes in the early universe.

Keywords: galaxies: dwarf — galaxies: photometry — galaxies: evolution

1. INTRODUCTION

Ultra-diffuse galaxies (UDG; van Dokkum et al. 2015), characterized by effective radii comparable to that of the Milky Way but with 100-1,000 times fewer stars, have garnered significant attention due to their unique properties and elusive formation mechanisms. UDGs are ubiquitously distributed throughout galaxy clusters, groups, and low-density environments. Similar to conventional dwarf galaxies, a substantial number of UDGs residing in galaxy clusters and groups present nuclear star clusters (NSC; e.g., Yagi et al. 2016; Lambert et al. 2024; Marleau et al. 2021; Rong et al. 2019). It has been postulated that certain ultra compact dwarfs (UCDs) may be the remnants of nucleated UDGs after tidal stripping (Mihos et al. 2017; Janssens et al. 2017, 2019).

The formation mechanism of UDGs remains enigmatic. Cosmological simulations offer insights into a high-spin UDG formation scenario (Amorisco & Loeb 2016; Rong et al. 2017; Liao et al. 2019; Benavides et al. 2023), indicating

that UDGs may acquire heightened specific angular momenta from their high-spin halos, a hypothesis supported by certain observational evidence (e.g., Rong et al. 2024a; Rong et al. 2020c). However, zoom-in hydrodynamical simulations suggest an outflow model as a potential alternative to the high-spin model, proposing that the internal feedback from supernovae is relatively weak compared to typical dwarf galaxies. Under this model, feedback-driven outflows weaken central gravitational potentials, leading to outward migration of stars and dark matter, ultimately forming an extended stellar disk (e.g., Di Cintio et al. 2017; Chan et al. 2018; Cardona-Barrero et al. 2020).

In addition to these prominent formation models, a study by Mancera Piña et al. (2020) suggests an alternative scenario where UDGs exhibit comparable halo spin but a higher angular momentum conversion factor compared to typical dwarf galaxies. Furthermore, Wright et al. (2021) propose that UDGs may arise from the merger of dwarf galaxies, with a hypothesis of transient amplification of descendant halos’ spin during merging events to replicate UDGs.

In high-density environments, UDGs may also arise from typical dwarf galaxies through tidal interactions with massive galaxies (Carleton et al. 2019; Jiang et al. 2019), or via ram-pressure stripping (Grishin et al. 2021). These formation sce-

narios of UDGs in high-density regions are further supported by spectroscopic investigations of UDG kinematics, revealing minimal rotational motion in UDGs (e.g., [Chilingarian et al. 2019](#); [van Dokkum et al. 2019b](#)).

Furthermore, [van Dokkum et al. \(2015\)](#) propose a failed L^* galaxy (FLG) formation model for UDGs, suggesting that UDGs inhabit L^* -type massive dark matter halos but exhibit diminished stellar mass due to environmental influences during the early epochs of the universe ([Yozin & Bekki 2015](#)).

Indeed, UDGs located in high-density regions, such as galaxy clusters, were previously thought to be enclosed by substantial dark matter halos to shield them from tidal disruption, potentially representing FLGs. Notably, the largest UDG in the Coma cluster, DF44, was initially inferred to harbor a dark matter halo mass of $10^{12} M_{\odot}$ ([van Dokkum et al. 2016](#)), based on the dynamics of member globular clusters (GCs). However, subsequent assessments of halo mass using stellar disk kinematics have cast doubt on this assumption of a massive halo ([van Dokkum et al. 2019b](#)).

Further statistical analyses of UDG samples, utilizing the number/mass of GCs and weak lensing, suggest that the majority of UDGs in galaxy clusters possess masses akin to typical dwarf galaxies ($\sim 10^{11} M_{\odot}$), contrasting with the mass of the Milky Way ([Sifón et al. 2018](#); [Peng & Lim 2016](#)). Additionally, spectroscopic observations of GCs in two UDGs within the NGC1052 galaxy group reveal the absence of dark matter components within these UDGs ([van Dokkum et al. 2018, 2019a](#)). Current understanding leans towards UDGs residing in low-mass halos rather than massive ones, with some studies proposing that UDGs are an extension of dEs/dSphs rather than a distinct class of galaxies (e.g., [Zöller et al. 2024](#); [Venhola et al. 2017](#); [Conselice 2018](#)).

If UDGs indeed exist in low-mass halos, they may exhibit a (thick) disk-like morphology with Sérsic indices of $n \lesssim 1$ ([Leisman et al. 2017](#); [Rong et al. 2020b](#); [Rong et al. 2024b](#); [van der Burg et al. 2016](#)), with or without a central NSC. However, the presence of a bulge-like structure with significant size in their central regions, a feature commonly observed in massive galaxies ([Kormendy et al. 2010](#); [Kormendy & Bender 2012](#)), is unexpected in UDGs. In this study, we present, for the first time, a serendipitous sample of UDGs showcasing central pseudo-bulges. This novel finding may add complexity to the understanding of UDG halo masses and formation mechanisms. In section 2, we introduce observational data and highlight a cohort of UDGs displaying pseudo-bulge structures at their cores, surrounded by extremely faint and expansive stellar disks. Section 3 delves into the potential formation mechanism of this specific UDG subgroup. Our conclusions are encapsulated in section 4. Throughout this paper, we employ “log” to represent “ \log_{10} ”.

2. HI-BEARING UDGs WITH PSEUDO-BULGES

2.1. Sample and optical photometry

Our sample is derived from the Arecibo Legacy Fast Alfa Survey (ALFALFA; [Giovanelli et al. 2005](#); [Haynes et al. 2018](#)), a comprehensive extragalactic HI survey spanning approximately $6,600 \text{ deg}^2$ in high Galactic latitudes. These HI

sources have been cross-referenced with optical data from the Sloan Digital Sky Survey (SDSS DR12; [Alam et al. 2015](#)). Exploiting the increased depth of the recent DESI Legacy Imaging Surveys ([Dey et al. 2019](#)), we conducted a comparative analysis of the SDSS and DESI images of these HI samples, resulting in the detection of a dwarf galaxy, AGC238976. While AGC238976 appears as a point source in the SDSS images, the DESI images reveal a subtle stellar disk at the galaxy’s periphery.

Illustrated in Fig. 1, AGC238976 displays a prominent central nuclei-like structure, potentially indicative of a small bulge or NSC, alongside a faint outer disk component. The disk component is particularly discernible in the g - and r -bands, but less pronounced in the z -band. Notably, spiral arm-like structures are also discernible within the disk component.

Following a methodology akin to that outlined in [Chen et al. \(2022\)](#), we employ a ‘double-Sérsic’ model combined with a ‘sky’ model to fit the g , r , and z -band DESI DR9 images of AGC238976 using the GALFIT software. The two Sérsic models represent the central nuclei-like structure and the outer disk, respectively. Throughout the fitting procedure, the point spread function (PSF) image for each band is utilized to deconvolve the corresponding galactic image, facilitating the precise determination of the effective radius of AGC238976’s central nuclei-like structure. The optimal parameters of the double-Sérsic model are presented in Table 2.1.

[Chen et al. \(2022\)](#) have demonstrated that a point-like structure with an effective radius exceeding $1/3$ of the Full Width at Half Maximum (FWHM) of the PSF can be accurately modeled through fitting. In our analysis of AGC238976, we observe effective radii R_h for the central nuclei-like structure of 0.96, 1.12, and 1.03 arcsec in the g , r , and z -bands, respectively. These values surpass the FWHM of the PSF, which are approximately 1.29, 0.94, and 0.89 arcsec for g , r , and z -bands, respectively, enabling precise measurements. This also suggests the presence of a central bulge in AGC238976 with $R_h \sim 500 \text{ pc}$, rather than a NSC or GC with $R_h \sim 3 - 100 \text{ pc}$, as depicted in panel a of Fig. 2. Considering AGC238976’s classification as a dwarf galaxy with a stellar mass of $10^{8.38} M_{\odot}$ ([Durbala et al. 2020](#)), identification of a bulge at its core is particularly intriguing.

The outer disk of AGC238976 exhibits a substantial effective radius of around 7 kpc and an extremely low surface brightness, characterized by an r -band mean surface brightness within the effective radius of $\langle \mu \rangle_{h,d} \sim 27 \text{ mag/arcsec}^2$, meeting the selection criteria for UDGs ([van Dokkum et al. 2015](#); [van der Burg et al. 2016](#)). Therefore, we propose that AGC238976 could be classified as a UDG with a central bulge.

Our subsequent investigation entails a search within the ALFALFA catalog for dwarf galaxies resembling AGC238976, characterized by distinct central nuclei-like sources suggestive of NSCs or minor bulge structures, surrounded by faint stellar disk components. Employing a fitting strategy akin to that of AGC238976, we meticulously

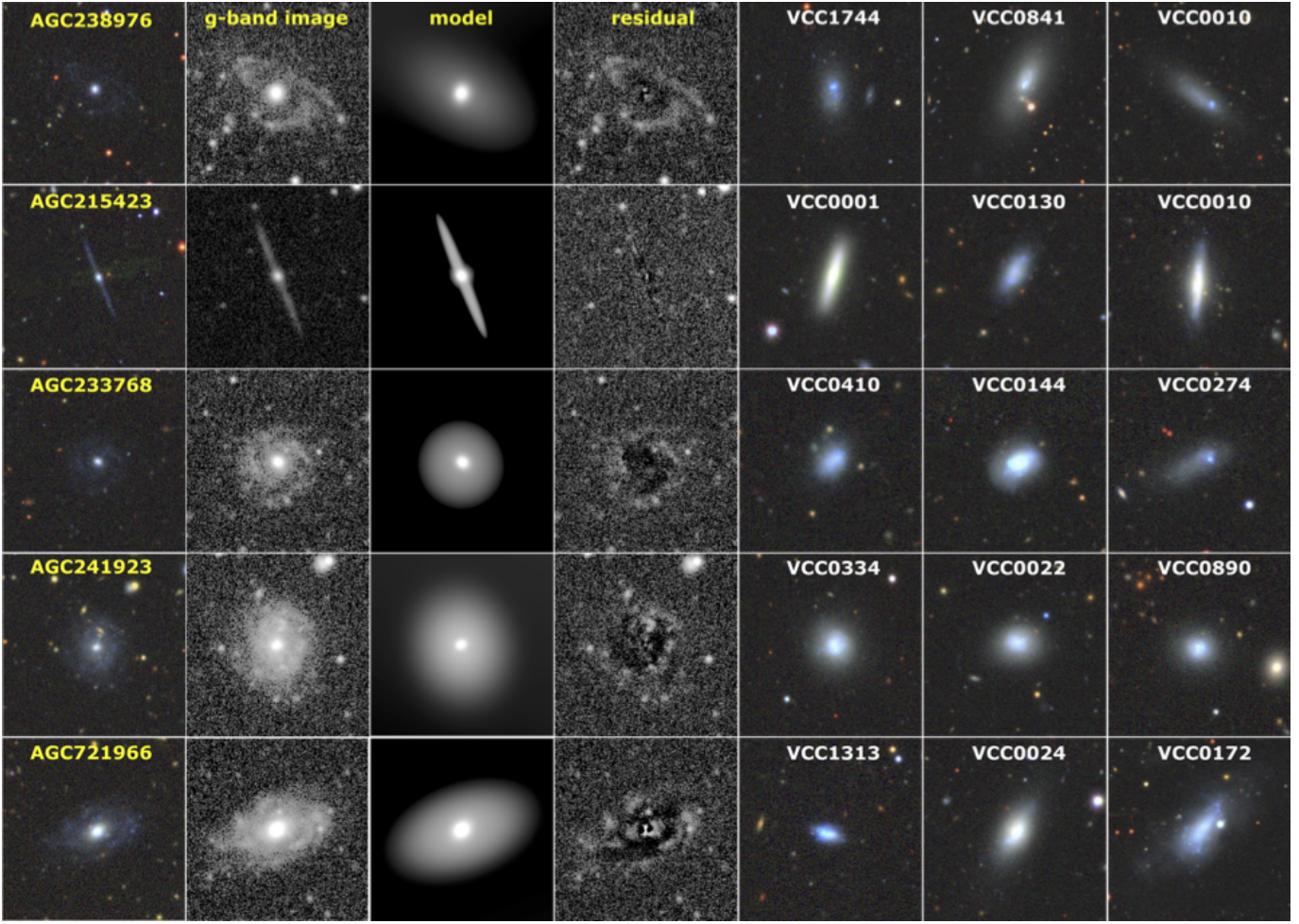


Figure 1. The left four columns of panels depict images of the five chosen UDGs with bulges. The panels, from left to right, display the colored DECaLS images, g -band images, double-Sérsic profile fitting outcomes, and residuals. The right three columns of panels showcase DESI images of 15 BCD examples from Meyer et al. (2014) for comparison.

analyze their optical images using a ‘double-Sérsic’ profile. The criteria for identifying analogous galaxies are as follows:

(1) The galaxy’s stellar mass should not exceed $10^9 M_{\odot}$. Previous studies by Durbala et al. (2020) involved stellar mass estimations of ALFALFA galaxies through three methods: UV-optical-infrared SED fitting, SDSS $g - i$ color, and W_2 magnitude. Preference is given to the stellar mass derived from SED fitting. In cases where UV or infrared data are unavailable for SED fitting, leading to an inability to estimate the stellar mass, the stellar mass is determined based on the $g - i$ color. Any discrepancies in stellar mass obtained from these methods are considered insignificant.

(2) The effective radius of the central nuclei-like structure should range from 1/3 FWHM of the PSF to 600 pc in the g , r , and z -bands of the DESI survey. This range aligns with the compact systems selection criterion detailed in Chen et al. (2022). The publicly available distance provided by the ALFALFA team (Haynes et al. 2018) is utilized to calculate the effective radius of each HI-bearing galaxy.

(3) The effective radius $R_{h,d}$ of the disk component should exceed 1.5 kpc, with the mean surface brightness within

$R_{h,d}$ in the r -band, $\langle \mu \rangle_{h,d}$, not exceeding approximately 24 mag/arcsec^2 . This criterion is instrumental in identifying UDGs (van Dokkum et al. 2015; van der Burg et al. 2016).

Only 5 UDGs with central nuclei-like components have been discovered from the parent sample with totally 8,600 member dwarf galaxies, with AGC238976 being one of them. The photometric results of these five galaxies are elaborated in Table 2.1, and their DESI images are presented in Fig. 1. The effective radii of the central nuclei-like components in all five UDGs significantly surpass the typical range of NSCs, UCDs, and GCs, which typically have effective radii ranging from approximately 3 pc and 100 pc (Walcher et al. 2006; Georgiev et al. 2016; Spengler et al. 2017; Neumayer et al. 2020; Hilker et al. 1999; Drinkwater et al. 2000), as illustrated in panel a of Fig. 2. Therefore, these nuclei-like components are identified as bulges within UDGs rather than NSCs.

Moreover, using the methodology outlined by Rong et al. (2024a), we have calculated the distances of these five UDGs from their nearest galaxy clusters and groups. Importantly, all these UDGs are located beyond three times the virial radii

of the galaxy clusters/groups, indicating their isolation from the gravitational influence of these large-scale structures or other galaxies. Hence, the distance measurements of these galaxies are minimally affected by their peculiar velocities. Consequently, these UDGs are also unlikely to be massive late-type galaxies situated at greater distances, as any misinterpretation of their distances could lead to their misclassification as UDGs. In summary, a cohort of UDGs with central bulges has indeed been identified within the ALFALFA sample.

Additionally, it is noteworthy that the Sérsic indices of the bulge components are below 2.5, indicating a potential classification as pseudo-bulges (Kormendy & Kennicutt 2004). The Sérsic indices of the outer stellar disks are below 1, akin to typical isolated UDGs documented by Leisman et al. (2017) and Rong et al. (2020a).

On the color versus stellar mass diagram, the outer stellar disks occupy the bluest sector of the ‘blue cloud’, as illustrated in panel b of Fig. 2, indicating young stellar populations within the stellar disks. Furthermore, these outer disks exhibit spiral-like features, suggesting recent gas accretion and star formation within the stellar disks. The central bulges display relatively redder colors compared to the blue outer disks, with the exception of AGC233768 (where the colors of the bulge and disk are comparable, with $g-r \sim 0.3$ mag), indicating a possible recent quenching or rejuvenation process in the bulges. In essence, these pseudo-bulges are anticipated to have formed earlier than the outer disk components.

2.2. HI detection

In the left panels of Fig. 3, we present the ALFALFA HI spectra for the five UDGs, with W_{50} representing the 50% peak widths of the HI lines. In galaxies exhibiting substantial rotation and a relatively large inclination (i.e., small apparent axis ratio $b/a \ll 1$), the HI spectrum is expected to display a double-horned profile with sharp edges on both sides of the HI line (El-Badry et al. 2018). In such cases, W_{50} is primarily influenced by the rotation velocity. Conversely, for galaxies with a large apparent axis ratio and low inclination, the HI spectrum should exhibit a single-horned profile, and W_{50} should encapsulate information about both the rotation velocity and velocity dispersion, with a potential dominance of velocity dispersion. However, our five UDGs consistently display double-horned HI spectra, despite the small (optical) inclinations with $b/a \sim 0.9$ observed in the disk components of AGC233768 and AGC241923. This implies that the rotation of gas, and consequently the disk components, in these UDGs are notably significant.

For our five UDGs, we estimate their rotation velocities V_{rot} as $V_{\text{rot}} \simeq W_{50}/2/\sin\phi$, where ϕ represents the HI inclination, and W_{50} is corrected for instrumental broadening (Haynes et al. 2018). In the absence of resolved HI data, we estimate the HI disk inclination ϕ using the average b/a ratio from the g , r , and z -bands, with $\sin\phi = \sqrt{(1 - (b/a)^2)/(1 - q_0^2)}$ (if $b/a \leq q_0$, $\phi = 90^\circ$), where q_0 denotes the intrinsic thickness of a galaxy.

Coincidentally, among the UDGs with pseudo-bulges, one galaxy, AGC215423, is observed in an edge-on orientation (Fig. 1), showcasing an exceptionally slim stellar disk with $q_0 \lesssim 0.1$. To maintain uniformity, we adopt $q_0 \simeq 0.1$ for all five UDGs to determine their rotation velocities, which are summarized in Table 2.1.

We further compare the rotation velocities of the five UDGs with those of other HI-bearing dwarf galaxies of similar stellar masses in ALFALFA. Employing an average intrinsic thickness of $q_0 \simeq 0.2^1$ for the HI-bearing galaxies (Tully et al. 2009; Giovanelli et al. 1997; Li et al. 2022), we estimate their rotation velocities. As illustrated in the insets of Fig. 3, the rotation velocities of the five UDGs are relatively high compared to the broader sample of HI-bearing dwarfs within the stellar mass range of $8 < \log M_{\text{st}}/M_\odot < 9$, potentially indicating the presence of massive halos or high spins in these UDGs (Mo et al. 1998; Rong et al. 2024a).

3. DISCUSSION

3.1. Are these galaxies exceptional?

Dwarf galaxies with bulges are not rare. One notable subset is the blue compact dwarf galaxies (BCDs), characterized by high interstellar matter density, vigorous star formation activity, small effective radii (Janowiecki & Salzer 2014; Meyer et al. 2014) and low Sérsic indices $n < 2.5$ (Lian et al. 2015; Chen et al. 2022). Observations have revealed that a significant proportion of BCDs feature stellar disks, often referred to as ‘‘hosts’’, with low surface brightness (LSB; Meyer et al. 2014) or the accretion of gas leading to the formation of HI disks (e.g., Tang et al. 2022). Hence, from a structural standpoint, both BCDs and the five selected UDGs exhibit bulge-like structures and outer faint disks, showcasing similarities.

Nevertheless, a comparison between the outer disk components of our five sources and the LSB hosts of BCDs, as depicted in panels c and a of Fig. 2, reveals that the outer disk components of our UDGs are considerably larger and fainter than those of the LSB hosts of BCDs, bearing a closer resemblance to UDGs. Furthermore, a visual inspection of the morphologies presented in Fig.1 highlights distinct differences between BCDs and our five UDGs.

Regarding UDGs, while some UDGs have been identified to host NSCs in their centers, the presence of pseudo-bulges in the central regions of UDGs remains unreported. However, there is growing evidence suggesting that distinct populations of UDGs with likely different formation pathways exist (Buzzo et al. 2024; Jones et al. 2023). Hence, the characteristics exhibited by the five UDGs we have uncovered appear to be distinctly unique, whether viewed through the lens of BCDs or UDGs.

¹ Based on the findings of (Rong et al. 2024b), the intrinsic thickness of young stellar population components, which reflect the gas distributions in dwarf galaxies, may be thicker, with $q_0 \sim 0.4$. Using $q_0 \sim 0.4$ or $q_0 \sim 0.2$ for the parent sample would not alter our conclusion.

AGC	Dist. [Mpc]	$\log M_{\text{st}}$ [$\log M_{\odot}$]	$\log M_{\text{HI}}$ [$\log M_{\odot}$]	W_{50} [km/s]	Inc. [deg]	V_{rot} [km/s]	Band	Comp.	Mag. [mag]	R_{h} [kpc]	μ_0 [mag/arcsec ²]	n	b/a	P.A. [deg]	χ^2/dof	
238976	105.4±2.3	8.38±0.03	9.85±0.05	183±3	69.9 ^{+13.7} _{-12.8}	97.5 ^{+13.3} _{-6.9}	<i>g</i>	disk	19.31	6.75	26.15	0.78	0.55	57.6	0.587	
								bulge	18.62	0.43	19.00	1.07	1.0	-6.6		
							<i>r</i>	disk	19.40	7.67	26.95	0.48	0.37	54.0		0.710
								bulge	18.11	0.53	18.34	1.41	0.98	18.5		
							<i>z</i>	disk	20.17	8.66	28.31	0.06	0.15	51.1		0.792
								bulge	17.90	0.56	18.69	1.16	0.96	-19.9		
215423	91.8±2.3	8.03±0.06	9.40±0.06	175±22	90.0	87.5 ^{+11.0} _{-11.0}	<i>g</i>	disk	19.24	6.69	27.12	0.10	0.07	21.6	0.655	
								bulge	18.89	0.34	18.92	1.15	0.84	36.3		
							<i>r</i>	disk	19.27	6.48	27.08	0.06	0.06	21.6	0.730	
								bulge	18.37	0.41	16.36	2.45	0.88	19.4		
							<i>z</i>	disk	19.13	5.95	27.60	0.15	0.07	22.7	0.806	
								bulge	18.33	0.42	18.96	1.07	0.68	19.9		
233768	115.2±2.4	8.44±0.06	9.31±0.05	60±6	22.2 ^{+7.5} _{-8.0}	79.4 ^{+55.6} _{-24.9}	<i>g</i>	disk	18.85	4.29	25.10	0.35	0.97	24.4	0.639	
								bulge	18.73	0.52	18.30	1.64	0.84	43.8		
							<i>r</i>	disk	18.50	4.25	24.18	0.75	0.94	6.80	0.714	
								bulge	18.44	0.51	18.43	1.39	0.78	55.22		
							<i>z</i>	disk	17.87	8.08	21.73	2.51	0.87	-40.9	0.799	
								bulge	18.20	0.55	17.98	1.59	0.72	52.32		
241923	86.7±2.4	8.75±0.05	9.32±0.05	86±6	34.1 ^{+4.9} _{-4.4}	76.7 ^{+16.1} _{-13.1}	<i>g</i>	disk	17.56	3.73	23.80	0.60	0.84	10.7	0.518	
								bulge	19.35	0.43	20.86	0.63	0.83	-59.8		
							<i>r</i>	disk	17.22	3.60	23.33	0.64	0.87	7.4	0.556	
								bulge	18.83	0.43	20.13	0.77	0.98	-66.5		
							<i>z</i>	disk	17.07	3.67	23.22	0.64	0.78	1.7	0.704	
								bulge	18.61	0.48	20.13	0.78	0.76	-77.3		
721966	78.9±2.3	8.59±0.06	9.35±0.06	196±5	55.4 ^{+1.6} _{-1.2}	119.0 ^{+4.8} _{-5.2}	<i>g</i>	disk	17.79	4.59	24.98	0.37	0.58	-70.0	0.494	
								bulge	17.23	0.40	15.89	2.25	0.74	-43.0		
							<i>r</i>	disk	17.78	4.69	25.14	0.26	0.59	-70.2	0.595	
								bulge	16.79	0.60	16.62	2.10	0.72	-54.3		
							<i>z</i>	disk	17.62	4.45	24.63	0.47	0.55	-76.1	0.724	
								bulge	16.62	0.62	16.92	1.89	0.69	-53.0		

Table 1. Properties of five UDGs with pseudo-bulges. Col. (1): ALFALFA name; Col. (2): distance to us; Col. (3): stellar mass (Durbala et al. 2020); Col. (4): HI mass; Col. (5): 50% peak width of HI line; Col. (6): inclination; Col. (7): rotation velocity; Col. (8): photometry bands g , r , and z ; Col. (9): bulge or disk components; Col. (10): apparent magnitude corrected for the Galactic extinction; Col. (11): effective radius; Col. (12): central surface brightness; Col. (13): Sérsic index; Col. (14): axis ratio; Col. (15): position angle; Col. (16): normalized χ^2 .

3.2. Formation of these UDGs with pseudo-bulges

One intriguing question pertains to the evolutionary mechanism behind the transition of these sub-luminous galaxies from a bulge-shaped structure in their early formation to a disk structure in more recent formations. Empirical galaxy formation models suggest that the likelihood of a galaxy adopting a disk structure is higher if its halo possesses a higher spin, whereas a halo with lower spin is more inclined to form a dense, compact structure resembling a bulge shape (e.g., Mo et al. 1998; van den Bosch 1998; Diemand et al. 2005; Desmond et al. 2017; Liao et al. 2019). Hence, the formation of bulges characterized by relatively older stellar populations is likely to occur within dark matter halos exhibiting low spin values, whereas the emergence of outer disks, distinguished by high rotation velocities, is expected within halos characterized by high spin values, thus presenting an inherent paradox.

One plausible explanation for this paradox suggests that BCD-like pseudo-bulges may have originated from galaxy-galaxy mergers (Bekki 2008). The merging of dwarf galaxies can induce central starbursts and give rise to massive compact cores dominated by young stellar populations. Meanwhile, the older stellar components in the precursor dwarf galaxies may transform into diffuse, LSB components post-merger (Bekki 2008). However, this scenario suggests that the compact cores are likely to be characterized by younger

(bluer) stellar populations and embedded within older (redder) disks with a more diffuse spatial distribution. This model provides a potential explanation for the formation of AGC233768, where the outer disk (with $g - r \sim 0.35$ mag) displays a slightly redder hue than the central bulge (with $g - r \sim 0.29$ mag), contrasting with the other four galaxies where the pseudo-bulges are redder, and therefore older, than the outer disks.

Alternatively, we suggest that during the merging phase, the two dark matter halos may have contained minimal or no stars but abundant gas reservoirs. As a result, the merging of the gas components from the two halos could have initiated starbursts, leading to the formation of compact pseudo-bulges without an accompanying old stellar disk. Subsequently, any remaining gas would likely have been expelled from the merged galaxy post-merger due to stellar or AGN feedback mechanisms activated by the merging event.

Concurrently, the significant spin of the halo in the progeny galaxy following the merger, derived from the orbital angular momentum of the merging system, provides an explanation for the heightened rotation velocities observed in our five UDGs. Recently, these bulge-like galaxies have experienced a renewed influx of gas from the neighboring environment (Chandola et al. 2023), inheriting the high spin of their halos, reigniting the star formation process, and facilitating the formation of thin stellar disks.

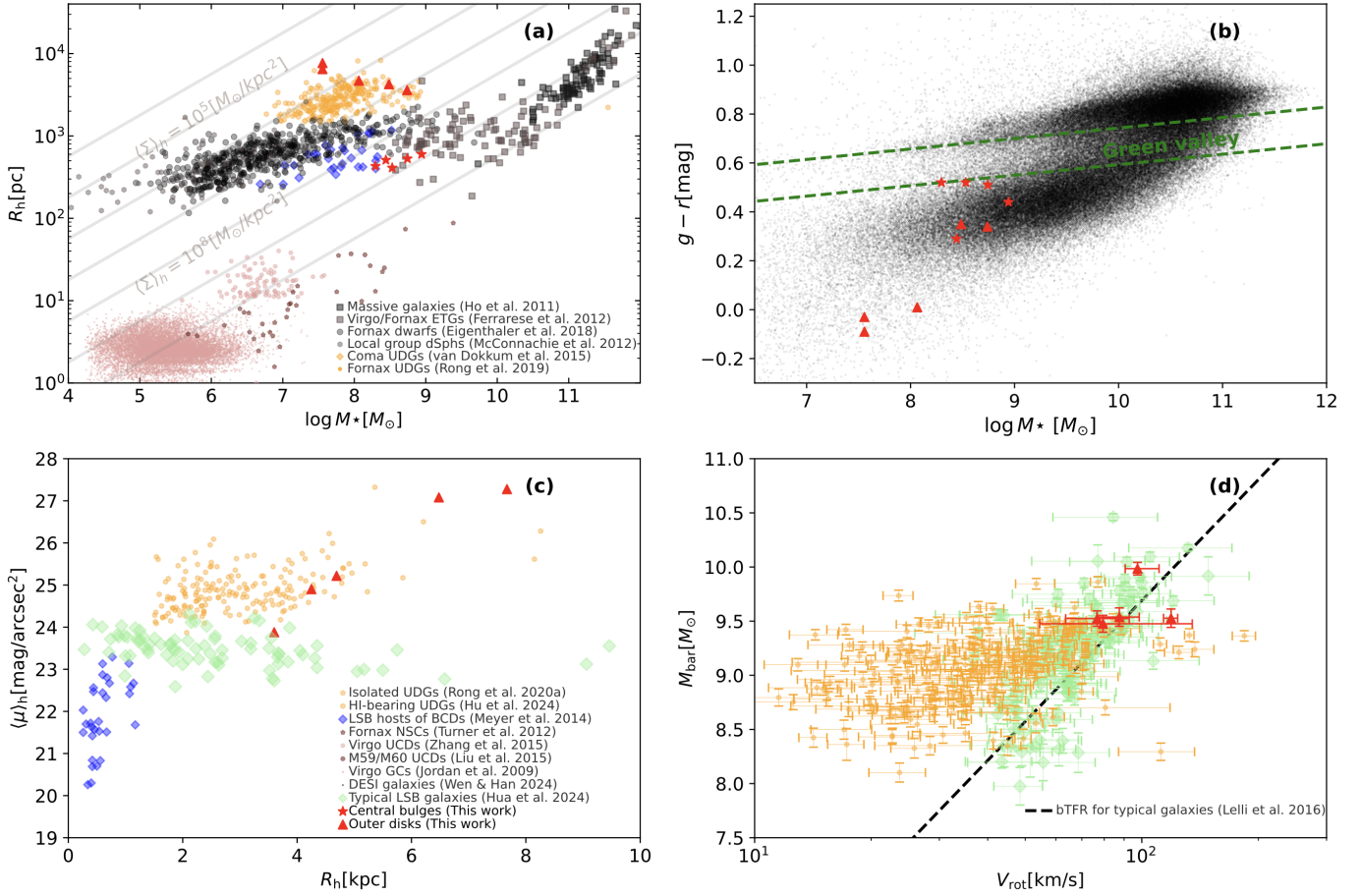


Figure 2. a) Stellar mass-size relationship for galaxies and globular clusters, including UDGs. b) Color-stellar mass diagram for DESI galaxies with radial velocities $v < 18,000$ km/s, based on data from Wen & Han (2024). c) Comparison of effective radius $R_{h,d}$ versus r -band mean surface brightness $\langle \mu \rangle_{h,d}$ for the outer disk components of the five chosen UDGs (red), the LSB hosts of typical BCDs from (Meyer et al. 2014, blue), the stellar disks of typical UDGs from (Hu et al. 2023, black), and the stellar disks of typical LSB galaxies from (Hua et al. 2024, light-green). d) Comparison of baryonic Tully-Fisher relation (bTFR) for the five chosen UDGs hosting pseudo-bulges (red), typical UDGs (Hu et al. 2023, orange), as well as typical LSB galaxies (Hua et al. 2024, light-green). The black dashed line depicts the best-fit bTFR for typical galaxies by Lelli et al. (2016). In these panels, the central bulge and outer disk components of the five selected UDGs are represented by red stars and triangles, respectively. The stellar masses of the bulge and disk components of the chosen UDGs are derived from mass-to-light ratios of Bell et al. (2003), with $\log(M_*/L_*)_g = 1.519 \times (g - r) - 0.499 - 0.093$, adjusting the masses by 0.093 dex to transition from a “diet” Salpeter to Chabrier initial mass function (Gallazzi et al. 2008).

However, this theoretical framework faces a potential limitation, as it presupposes that the precursor halos of the merging galaxies must harbor gas while being devoid of or possessing minimal stars, a condition that remains uncertain in cosmological simulations. Additionally, if the five selected UDGs exhibit higher spins, their positions on the baryonic mass versus rotation velocity diagram may significantly differ from the baryonic Tully-Fisher relation (bTFR) observed in typical galaxies (Lelli et al. 2016), but align with that of typical UDGs (Rong et al. 2024a; Hu et al. 2023). As shown in panel d of Fig. 2, due to the small sample size, we are unable to determine whether these five UDGs adhere to the bTFR of typical galaxies or UDGs.

Moreover, we cannot dismiss the alternative scenario that these UDGs might be ensconced within substantial dark mat-

ter halos, consequently contributing to their augmented rotation velocities. To ascertain the halo mass of these UDGs, resolved HI observations and gas velocity mappings are imperative. Should these UDGs be confirmed to inhabit massive halos while maintaining stellar masses akin to typical dwarf galaxies, they could potentially represent the “failed L^* galaxies” proposed by van Dokkum et al. (2015). The pseudo-bulges observed in these ultra-diffuse galaxies may have originated from intense early AGN feedback, potentially leading to the cessation of subsequent star formation and the formation of sub-luminous galaxies. Furthermore, the early strong AGN feedback also hints at the possibility of higher central black hole masses in these UDGs compared to conventional dwarf galaxies. This scenario bears resemblance to the recent discovery by the JWST telescope of high-

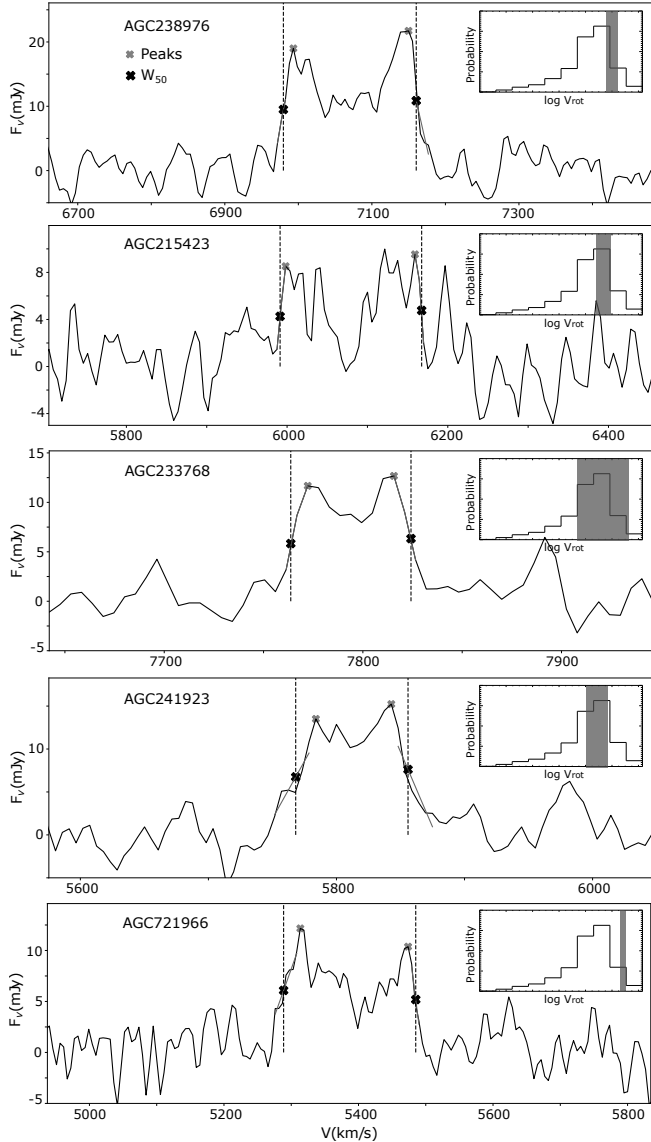


Figure 3. HI spectra of the 5 UDGs with bulges from ALFALFA are presented. Each panel displays the positions used for calculating W_{50} for the respective galaxy. The inset in each panel compares the rotation velocity (with the gray region indicating the 1σ uncertainty range, estimated from the errors of W_{50} and inclination.) of the galaxy with the rotation velocity distribution (shown as a black histogram) of all HI-bearing dwarf galaxies with $8 < \log M_{st}/M_{\odot} < 9$ in ALFALFA.

redshift “little red dots” (Matthee et al. 2024), characterized by compact nuclei-like structures and a higher prevalence of central black hole masses relative to galaxies of equivalent stellar mass (Durodola et al. 2024). In this context, the five UDGs we have identified may represent the descendants of “little red dots”.

4. CONCLUSION

By analyzing the images of the ALFALFA dwarf galaxies from the DESI Legacy Imaging Survey, we have iden-

tified five dwarf galaxies featuring central pseudo-bulges. These galaxies display blue pseudo-bulges with Sérsic indices $n < 2.5$ and effective radii spanning 300-700 pc, along with bluer thin stellar disks exhibiting low surface brightness and expansive effective radii that align with the UDG definition. We compare the properties of their disk components with the LSB hosts of BCDs and stellar disks of typical UDGs, and find the outer disk components resemble UDGs more closely. These galaxies are thus referred as UDGs with pseudo-bulges.

The rotation velocities of these UDGs, determined through calculations utilizing HI line widths and optical inclinations, are relatively high compared to those of typical dwarf galaxies of equivalent mass, suggesting the presence of high halo spins or substantial halos.

We propose two potential formation models for these UDGs. Firstly, they are likely formed from the merger of dwarf galaxies which lacked old stars in the progenitors, resulting in a central bulge-shaped structure, while concurrently enhancing their halo spin. Subsequent accretion of surrounding gas facilitates the formation of extended stellar disk.

Secondly, it is also plausible that these UDGs could represent “failed L^* galaxies” with massive dark matter halos but significantly reduced star formation efficiencies. It is possible that intense AGN feedback is necessary to account for the low star formation efficiency and bulge-shaped structures of these galaxies, suggesting the presence of overmassive central black holes relative to their host galaxies in the early universe. If this scenario holds true, then the five UDGs may be viewed as descendants of the “little red dots” discovered by JWST.

1 We thank Wen, Zhong Lue at NAOC for data. YR ac-
2 knowledges supports from the NSFC grant 12273037, the
3 CAS Pioneer Hundred Talents Program (Category B), the
4 USTC Research Funds of the Double First-Class Initia-
5 tive, and the research grants from the China Manned Space
6 Project (the second-stage CSST science projects: “Investi-
7 gation of small-scale structures in galaxies and forecasting
8 of observations” and “CSST study on specialized galaxies
9 in ultraviolet and multi-band”). HXZ acknowledges support
10 from the NSFC grant 11421303. QG is supported by the
11 National SKA Program of China No. 2022SKA0110201,
12 the CAS Project for Young Scientists in Basic Research
13 Grant No. YSBR-062, and the European Union’s Horizon
14 2020 Research and Innovation Programme under the Marie
15 Skłodowska-Curie grant agreement No. 101086388. HYW
16 is supported by the National Natural Science Foundation of
17 China (NSFC, Nos. 12192224) and CAS Project for Young
18 Scientists in Basic Research, Grant No. YSBR-062.

19 The Legacy Surveys consist of three individual and com-
20plementary projects: the Dark Energy Camera Legacy Sur-
21vey (DECaLS; Proposal ID #2014B-0404; PIs: David
22Schlegel and Arjun Dey), the Beijing-Arizona Sky Survey
23(BASS; NOAO Prop. ID #2015A-0801; PIs: Zhou Xu and
24Xiaohui Fan), and the Mayall z-band Legacy Survey (MzLS;
25Prop. ID #2016A-0453; PI: Arjun Dey). DECaLS, BASS
26and MzLS together include data obtained, respectively, at
27the Blanco telescope, Cerro Tololo Inter-American Observa-
28tory, NSF’s NOIRLab; the Bok telescope, Steward Observa-
29tory, University of Arizona; and the Mayall telescope, Kitt
30Peak National Observatory, NOIRLab. Pipeline processing
31and analyses of the data were supported by NOIRLab and
32the Lawrence Berkeley National Laboratory (LBNL). The
33Legacy Surveys project is honored to be permitted to conduct
34astronomical research on Iolkam Du’ag (Kitt Peak), a moun-
35tain with particular significance to the Tohono O’odham Na-
36tion.

37 NOIRLab is operated by the Association of Universities
38for Research in Astronomy (AURA) under a cooperative
39agreement with the National Science Foundation. LBNL is
40managed by the Regents of the University of California under
41contract to the U.S. Department of Energy.

42 This project used data obtained with the Dark Energy Cam-
43era (DECam), which was constructed by the Dark Energy
44Survey (DES) collaboration. Funding for the DES Projects
45has been provided by the U.S. Department of Energy, the
46U.S. National Science Foundation, the Ministry of Science
47and Education of Spain, the Science and Technology Fa-
48cilities Council of the United Kingdom, the Higher Edu-
49cation Funding Council for England, the National Center
50for Supercomputing Applications at the University of Illi-
51nois at Urbana-Champaign, the Kavli Institute of Cosmolog-
52ical Physics at the University of Chicago, Center for Cos-
53mology and Astro-Particle Physics at the Ohio State Uni-
54versity, the Mitchell Institute for Fundamental Physics and
55Astronomy at Texas A&M University, Financiadora de Es-
56tudos e Projetos, Fundacao Carlos Chagas Filho de Ampa-
57ro, Financiadora de Estudos e Projetos, Fundacao Car-
58los Chagas Filho de Amparo a Pesquisa do Estado do Rio
59de Janeiro, Conselho Nacional de Desenvolvimento Cien-
60tifico e Tecnológico and the Ministerio da Ciencia, Tecnolo-
61gia e Inovacao, the Deutsche Forschungsgemeinschaft and
62the Collaborating Institutions in the Dark Energy Survey.
The Collaborating Institutions are Argonne National Labora-

REFERENCES

- Alam, M. P. et al. 2015, *ApJS*, 219, 12
- Amorisco, N. C. & Loeb, A. 2016, *MNRAS*, 459, L51
- Bekki, K. 2008, *MNRAS*, 388, L10
- Bell, E. F., McIntosh, D. H., Katz, N., Weinberg, M. D. 2003, *ApJS*, 149, 289
- Benavides, J. A., Sales, L. V., Abadi, M. G., Marinacci, F., Vogelsberger, M., Hernquist, L. 2023, *MNRAS*, 522, 1033
- Buzzo, M. L., et al. 2024, *MNRAS*, 529, 3210
- Cardona-Barrero, S., Di Cintio, A., Brook, C. B. A., Ruiz-Lara, T., Beasley, M. A., Falcón-Barroso, J., Macciò, A. V. 2020, *MNRAS*, 497, 4282
- Carleton, T., Errani, R., Cooper, M., Kaplinghat, M., Penarrubia, J., Guo, Y. 2019, *MNRAS*, 485, 382
- Chan, T. K. et al. 2018, *MNRAS*, 478, 906
- Chandola, Y., Tsai, C. W., Li, D. 2023, *MNRAS*, 523, 3848
- Chen, G., Zhang, H.-X., Kong, X., Lin, Z., Liang, Z., Chen, Z., Tang, Y., Chen, X. 2022, *ApJL*, 934, 35
- Chilingarian, I. V., Afanasiev, A. V., Grishin, K. A., Fabricant, D., Moran, S. 2019, *ApJ*, 884, 79
- Conselice, C. J. 2018, *Research Notes of the American Astronomical Society*, 2, 43
- Desmond, H., Mao Y.-Y., Wechsler R. H., Crain R. A., Schaye J. 2017, *MNRAS*, 471, L11
- Dey, A., Schlegel, D. J., Lang, D., et al. 2019, *AJ*, 157, 168
- Di Cintio, A., Brook, C. B., Dutton, A. A., Maccio, A. V., Obreja, A., Dekel, A. 2017, *MNRAS*, 466, L1
- Diemand, J., Madau, P., Moore, B. 2005, *MNRAS*, 364, 367
- Drinkwater, M. J., Jones, J. B., Gregg, M. D., Phillipps, S. 2000, *PASA*, 17, 227
- Durbala, A., Finn, R. A., Crone Odekon, M., Haynes, M. P., Koopmann, R. A., O'Donoghue, A. A. 2020, *AJ*, 160, 271
- Durodola, E., Pacucci, F., Hickox, R. C. 2024, e-print arXiv:2406.10329
- Egenthaler, P., et al. 2018, *ApJ*, 855, 142
- El-Badry, K. et al. 2018, *MNRAS*, 477, 1536
- Ferrarese, L., et al. 2012, *ApJS*, 200, 4
- Gallazzi, A., Brinchmann, J., Charlot, S. and White, S. D. M. 2008, *MNRAS*, 383, 1439
- Georgiev, I. Y., Böker, T., Leigh, N., Lützgendorf, N., Neumayer, N. 2016, *MNRAS*, 457, 2122
- Giovanelli, R. et al. 2005, *AJ*, 130, 6
- Giovanelli, R. et al. 1997, *AJ*, 113, 22
- Grishin, K. A., Chilingarian, I. V., Afanasiev, A. V., Fabricant, D., Katkov, I. Y., Moran, S., Yagi, M. 2021, *Nature Astronomy*, 5, 1308
- Guo, Q., et al. 2011, *MNRAS*, 413, 101
- Guo, Q. et al. 2020, *Nature Astronomy*, 4, 246
- Haynes, M. P. et al. 2018, *ApJ*, 861, 49
- Herrmann, K. A., Hunter, D. A., Zhang, H.-X., Elmegreen, B. G. 2016, *Science*, 152, 177
- Hilker, M., Infante, L., Vieira, G., Kissler-Patig, M., Richtler, T. 1999, *A&AS*, 134, 75
- Ho, L. C., Li, Z.-Y. Barth, A. J., Seigar, M. S., Peng, C. Y. 2011, *ApJS*, 197, 21
- Hu, H.-J., Guo, Q., Zheng, Z., Yang, H., Tsai, C.-W., Zhang, H.-X., Zhang, Z.-Y. 2023, *ApJL*, 947, L9
- Hua, Z., Rong, Y., Hu, H. 2024, arXiv:2403.16754
- Hunter, D. A., et al. 2012, *AJ*, 144, 134
- Janowiecki, S., Salzer, J. J. 2014, *ApJ*, 793, 109
- Janssens, S., Abraham, R., Brodie, J., Forbes, D., Romanowsky, A. J., van Dokkum, P. 2017, *ApJL*, 839, 17
- Janssens, S., Abraham, R., Brodie, J., Forbes, D. A., Romanowsky, A. J. 2019, *ApJ*, 887, 92
- Jiang, F., Dekel, A., Freundlich, J., Romanowsky, A. J., Dutton, A. A., Maccio, A. V., Di Cintio, A. 2019, *MNRAS*, 487, 5272
- Jones, M. G., et al. 2023, *ApJL*, 942, 5
- Jordán, A., et al. 2009, *ApJS*, 180, 54
- Kormendy, J., Bender, R. 2012, *ApJS*, 198, 2
- Kormendy, J., Drory, N., Bender, R., Cornell, M. E. 2010, *ApJ*, 723, 54
- Kormendy, J., Kennicutt, R. C. J. 2004, *Annual Review of Astronomy & Astrophysics*, 42, 603
- Lambert, M., Khim, D. J., Zaritsky, D., Donnerstein, R. 2024, *AJ*, 167, 61
- Leisman, L., et al. 2017, *ApJ*, 842, 133
- Lelli, F., McGaugh, S. S., Schombert, J. M. 2016, *ApJL*, 816, L14
- Li, X., Shi, Y., Zhang, Z.-Y., Chen, J., Yu, X., Wang, J., Gu, Q., Li, S. 2022, *MNRAS*, 516, 4220
- Lian, J. H., Kong, X., Jiang, N., Yan, W., Gao, Y. L. 2015, *MNRAS*, 451, 1130
- Liao, S. et al. 2019, *MNRAS*, 490, 5182
- Liu, C., et al. 2015, *ApJ*, 812, 34
- Mancera Piña, P. E. et al. 2020, *MNRAS*, 495, 3636
- Marleau, F. R., Habas, R., Poulain, M., et al. 2021, *A&A*, 654, 105
- Matthee, J., Naidu, R. P., Brammer, G., et al. 2024, *ApJ*, 963, 129
- McConnachie, A. W. *AJ*, 144, 4
- Meyer, H. T., Lisker, T., Janz, J., Papaderos, P. 2014, *A&A*, 562, 49
- Mihos, J. C., Harding, P., Feldmeier, J. J., et al. 2017, *ApJ*, 834, 16
- Mo, H. J., Mao, S. D. & White, S. D. M. 1998, *MNRAS*, 295, 319
- Neumayer, N., Seth, A., Böker, T. 2020, *A&ARv*, 28, 4
- Peng, E., Lim, S. 2016, *ApJL*, 822, L31
- Rong, Y., Hu, H., He, M., Du, W., Guo, Q., Wang, H.-Y., Zhang, H.-X., Mo, H. 2024a, arXiv:2404.00555
- Rong, Y., He, M., Hu, H., Zhang, H.-X., Wang, H.-Y. 2024b, arXiv:2409.00944
- Rong, Y., Guo, Q., Gao, L., Liao, S., Xie, L., Puzia, T. H., Sun, S., Pan, J. 2017, *MNRAS*, 470, 4231

- Rong, Y., Zhu, K., Johnston, E. J., Zhang, H.-X., Cao, T., Puzia, T. H., Galaz, G. 2020a, *ApJL*, 899, L12
- Rong, Y., et al. 2020b, *ApJ*, 899, 78
- Rong, Y., Mancera Piña, P. E., Tempel, E., Puzia, T. H., De Rijcke, S. 2020c, *MNRAS*, 498, L72
- Rong, Y. et al. 2019, *ApJ*, 883, 56
- Sifón, C., van der Burg, R. F. J., Hoekstra, H., Muzzin, A., Herbonnet, R. 2018, *MNRAS*, 473, 3747
- Spengler, C., Côté, P., Roediger, J., et al. 2017, *ApJ*, 849, 55
- Tang, Y., et al. 2022, *A&A*, 668, 179
- Tully, R. B., Rizzi, L., Shaya, E. J., Courtois, H. M., Makarov, D. I., Jacobs, B. A. 2009, *AJ*, 138, 323
- Turner, M. L., Côté, P., Ferrarese, L., Jordán, A., Blakeslee, J. P., Mei, S., Peng, E. W., West, M. J. *ApJS*, 203, 5
- van den Bosch, F. C. 1998, *ApJ*, 507, 601
- van der Burg, R. F. J., Muzzin, A., Hoekstra, H. 2016, *A&A*, 590, A20
- van Dokkum, P. G., et al. 2015, *ApJL*, 798, L45
- van Dokkum, P. G. et al. 2016, *ApJL*, 828, L6
- van Dokkum, P. et al. 2018, *Nature Astronomy*, 555, 629
- van Dokkum, P. et al. 2019a, *ApJL*, 874, L5
- van Dokkum, P. et al. 2019b, *ApJ*, 880, 91
- Venhola, A., et al. 2017, *A&A*, 608, 142
- Walcher, C. J., Böker, T., Charlot, S., et al. 2006, *ApJ*, 649, 692
- Wen, Z. L., Han, J. L. 2024, *ApJS*, 272, 39
- Wright, A. C., Tremmel, M., Brooks, A. M., Munshi, F., Nagai, D., Sharma, R. S., Quinn, T. R. 2021, *MNRAS*, 502, 5370
- Yagi, M., Koda, J., Komiyama, Y., Yamanoi, H. 2016, *ApJS*, 225, 11
- Yozin, C. & Bekki, K. 2015, *MNRAS*, 452, 937
- Zhang, H.-X., et al. 2015, *ApJ*, 802, 30
- Zöllner, R., Kluge, M., Staiger, B., Bender, R. 2024, *ApJS*, 271, 52